C004

Fast-track Marine CSEM Processing and 3D Inversion

J.P. Morten* (EMGS) & A.K. Bjørke (EMGS)

SUMMARY

We present CSEM 3D inversion results where the receiver rotation angle relative to North is treated as a free parameter in the optimization. This allows us to omit receiver orientation estimation and data rotation pre-processing in the workflow. Moreover, the initial resistivity model is prepared independently from the CSEM data using available seismic and well log information. In this way, calibrated frequency domain data can be input directly to the anisotropic 3D inversion tool, with arbitrary initial values for the rotation angles. Synthetic data is generated using speed optimized modeling parameters. This demonstrates a fast-track 3D inversion workflow which can deliver a 3D inverted resistivity volume within few days after data has been uploaded from the vessel.

Introduction

Acquisition efficiency and capacity improvements in marine controlled source electromagnetic (CSEM) surveying have accommodated development from 2D lines to 3D grids. The number of data records in a state-of-the-art 3D CSEM survey can exceed 20 000, leaving analysis based on data or attribute inspection infeasible. Lower dimensional inversion approaches like 2.5D inversion (Hansen and Mittet, 2009) can only process the field measurements along the source towline compatible with the simplifying assumptions on model geometry. Full utilization of a 3D dataset can only be carried out through 3D modelling and inversion that can represent 3D effects measured by the combined inline and azimuth responses, i.e. data from receivers both on and off the source towline (Morten et al., 2009a). It was shown by Morten et al. (2009b) that the use of azimuth data puts stricter demands on the accuracy of the receiver rotation angle relative to the source dipole. We have extended a 3D inversion tool to determine these angles as part of the model reconstruction process incorporating azimuth data. This simplifies the data pre-processing as the rotation analysis can be omitted. Still, the disadvantages of 3D inversion approaches are long execution times and the necessity of a realistic initial background model. In the real data example shown in this paper, we utilize previously acquired seismic and well log information to create the initial model. Combined with a speed optimized modelling configuration, the workflow we outline below can facilitate a 3D inverted resistivity volume within few days after frequency domain data has been uploaded from the vessel.

3D inversion incorporating receiver orientation

The receiver orientation relative to the horizontal electric dipole source must be determined in order to describe the vector electromagnetic field measurements correctly. Specifically, the rotation angle relative to North is important for horizontal field components. Due to environmental noise and receiver parts interacting with the Earth magnetic field, conventional compass readings at the seabed are inaccurate. Therefore, such measurements may pose a problem when used for 3D inversion of azimuth data, since small errors in the rotation results in large data errors (Morten et al., 2009b). Gyroscopes provide accurate orientation measurements, but are currently too costly for large surveys.

Inversion approaches have been shown to give reproducible and robust estimates for the receiver rotation (Mittet et al., 2004; Key and Lockwood, 2009). We will now show how the 3D inversion tool described by Zach et al. (2008a) is extended to determine the receiver rotation in addition to the resistivity distribution. This allows us to omit the receiver rotation analysis in data pre-processing (Zach et al, 2008b), and use calibrated frequency domain data directly in the 3D inversion software. The gradient-based update module (Zhu et al., 1997) minimizes the squared L_2-norm of the misfit between observed and synthetic data, as well as any regularization terms. The data misfit term is given by

$$\epsilon_{\text{Data}}(\{\varphi\}, \boldsymbol{\rho}) = \sum_\alpha W_\alpha^2 \left| F_\alpha^{\text{Observed}} - F_\alpha^{\text{Synthetic}}(\varphi, \boldsymbol{\rho}) \right|^2 .$$

Here, $\{\varphi\}$ is the set of receiver rotation angles relative to North (heading), $\boldsymbol{\rho}$ is the inversion resistivity model, α denotes all indices needed to label each data sample e.g. frequency, field component, source-receiver point etc., F_α is an electric or magnetic field component, and finally W is a data weight incorporating information about the measurement uncertainty of the data sample (Morten et al., 2009b). Since all operations in the 3D inversion tool assume full 3D geometry, we work with un-rotated data, i.e. the measurements are represented in the frame of reference defined by the receiver sensor instruments on the seabed. We assume a locally flat seafloor, i.e. receiver pitch and roll are neglected. This is possible since the horizontal field components under investigation have low sensitivity to small tilt effects due to the much smaller magnitude of vertical field components.

The 3D inversion tool requires that the gradient of the misfit function with respect to all free parameters must be provided, including angles $\{\varphi\}$. For one receiver, the misfit gradient with respect to the unknown rotation angle is determined by the polar angle derivative operator in the plane,

$$\frac{\partial}{\partial \varphi} \begin{pmatrix} F_a(\varphi) \\ F_b(\varphi) \end{pmatrix} = \begin{pmatrix} F_b(\varphi) \\ -F_a(\varphi) \end{pmatrix},$$

where $F_{a,b}$ represents horizontal electric or magnetic field components in orthogonal directions a and b. This expression shows that the change in one data component from a change in rotation angle φ is determined by the data in the orthogonal component. Therefore, the azimuth data is of particular interest since the measurements are recorded at positions off the dipole field symmetry axis. Along the source towline symmetry axis, the electromagnetic fields will be predominantly unidirectional so that the derivative above varies monotonously with offset. For receivers off the towline on the other hand, the curvature of the measured electromagnetic field introduces variability of the horizontal data components that gives a stronger sensitivity to the receiver rotation. Another benefit of azimuth data is that the number of measurements in the dataset can easily increase by an order of magnitude. This is because the number of data points in a 3D dataset scales with the product of receivers by the number of towlines. Therefore, spurious noise effects become less significant.

We have argued that the inversion problem for receiver rotation angles benefits from using azimuth data in addition to line data, and that it is a well defined problem for a 3D inversion algorithm. This is also shown by the real data example below. We note that more powerful update schemes for the receiver rotation can be implemented with relative ease since the optimization problem for the rotation angle alone can be solved (Key and Lockwood, 2009), and also the higher order derivatives of the misfit function are readily computed.

Pre-survey resistivity model preparation

Gradient-based inversion approaches are to a large degree dependent on initial models that reflect the main background resistivity trends. A lot of effort is typically spent on the construction of the initial model before a reliable 3D inversion result can be obtained. Such initial models can be constructed using results from lower-dimensional inversion approaches that utilize more powerful update algorithms (Roth et al., 2007; Hansen and Mittet, 2009). A 3D model may then be constructed using interpolation of results from several locations, preferably incorporating 3D seismic horizons. Since the model building process can be time-consuming, 3D inversion is usually executed in the final stages of imaging and inversions. In order for 3D inversion to become useful as a fast-track imaging tool, it is therefore necessary to devise an initial model independently of the CSEM data. In such case, 3D inversion can be started immediately when the data has been uploaded from the vessel. As shown by Brevik et al. (2009), integrating seismic interval velocity models with well log data allows construction of a 3D resistivity model that may sufficiently reflect background resistivity trends. This process is independent of the CSEM data and may be carried out prior to the survey.
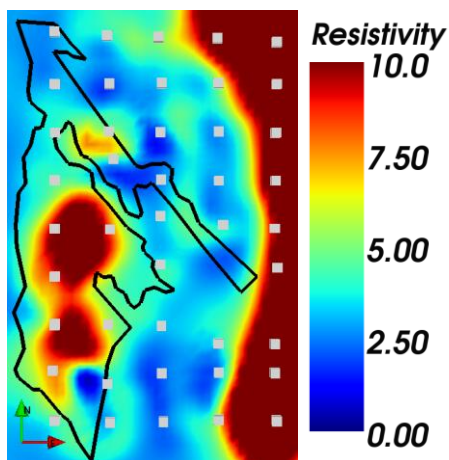

Figure 1 *Inversion vertical resistivity model at 1150 m below sea level. Receiver positions are indicated by grey rectangles, reservoir outline by black line. East: Troll western gas province.*
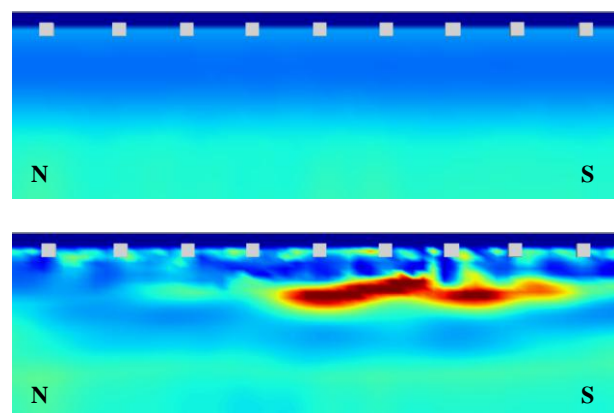
Figure 2 *Vertical section through westernmost North-South receiver line for initial vertical resistivity model (top) and final inversion model (bottom). Same colour scale as in Figure 1.*

Troll oil field inversion results

We have simulated the outlined fast-track 3D inversion workflow using data from a 2008 3D CSEM survey that was acquired in collaboration between Statoil and EMGS. The survey focused on thin hydrocarbon zones in the Troll western oil province in the North Sea outside Norway. The receiver and towline spacing were 1.25 km. A wealth of geophysical information for the area is available, but the only a priori information that was incorporated in this study is a seismic 3D interval velocity model and well logs from the area. For the inversions shown here, the resistivity model described by Brevik et al. (2009) was used as initial model for the horizontal component of the resistivity (ρ_H), and constant anisotropy ρ_V/ρ_H=2.0 based on general knowledge of the area was assumed to construct a vertical resistivity (ρ_V) model from the horizontal component. Care was taken to omit any use of the actual CSEM survey data while preparing the initial model. In Figure 2 (top) we show a section through the initial vertical resistivity model.

The inversion execution parameters were assigned default values and do not represent a setup specifically tailored to get a good result from this dataset. Thus no regularization or a priori constraints were applied, but as explained above seismic and well log information is embedded in the initial model. The results shown in Figures 1 and 2 are therefore representative of a first result that can be obtained from the calibrated frequency domain data prepared on the vessel. As such, these results cannot be expected to properly describe all aspects of the subsurface resistivity distribution, but form a starting point for further processing and interpretation work. In this example, we also show how the receiver rotation angles can be obtained in the inversion scheme. In a typical inversion project, a good estimate of the orientation has been obtained in the pre-processing. However, in this work the orientation of the receivers was considered unknown, and the arbitrary initial value 0.0 degrees was used for all angles {ϕ}. No bound for the possible values available to the optimization algorithm was applied. This means that the receiver rotation procedure of the data pre-processing could be omitted completely, thereby speeding up the total data processing time for fast-track application. In the inversion dataset we have included the horizontal electric field measurements of 44 receivers from 8 source towlines (5 North-South, 3 East-West) at the survey frequencies 0.25, 0.75, and 1.25 Hz. The final data fit was within the estimated uncertainty in the data.

In Figure 1 we show a depth slice of the vertical resistivity model from the anisotropic inversion result. As we can see, the extension of the oil reservoir agrees well with the seismic reservoir outline. Figure 2 shows a vertical section at the location of the oil field for the initial vertical resistivity model and the final inverted model. The depth of the oil field is about 300 m too shallow. The execution time for these results was 5 days (116.5 hours) with inversion settings optimized for speed. To this end, a very coarse scale modelling grid 200 m x 200 m x 110 m was used, and the computations were performed on 176 CPUs in parallel.
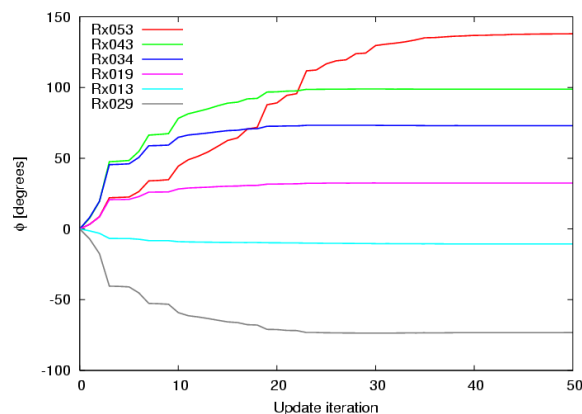

Figure 3 Evolution of receiver rotation angle with model updates. The final angle represents the receiver rotation with respect to North.

In Figure 3 we show the evolution of the angle ϕ for six random receivers from the survey. The final angles represent the rotation of the receiver on the seabed after free fall from the surface. We see that the angles converge on their final value within 40 updates, and that the updates seem to be defined by

stable minima of the inversion misfit function. Faster convergence could be obtained by using a more powerful update scheme for these parameters, or more accurate initial values. We have finally compared the angles obtained in the 3D inversion scheme to those obtained by an inline-data only rotation estimation method (Mittet et al., 2007) and find agreement within 5 degrees for most receivers.

Conclusions

We have demonstrated a 3D CSEM inversion workflow where the receiver rotation angles are unknowns along with the geomodel resistivity distribution. The gradient-based update scheme was able to recover the rotation angles correctly starting from arbitrary initial values. Thus the receiver rotation angle estimation could be omitted in the data pre-processing workflow. The initial anisotropic resistivity model was created independently from the CSEM data using available seismic and well log information, so that the calibrated frequency domain data could be utilized immediately in the 3D inversion software. We thereby obtain results representative of a fast-track 3D inversion workflow that could have been obtained within 5 days after the data was transferred from the vessel. Such fast-track results are important since they can quickly provide indications of prospective areas for more detailed surveying before the vessel has left the area. More generally the results quickly provide a starting point for the data interpretation workflow and more advanced inversion schemes involving specifically tailored initial models, regularizations, and constraints.

Acknowledgements

References

Brevik, I., Gabrielsen, P. T., and Morten, J. P. [2009] The role of EM rock physics and seismic data in integrated 3D CSEM data analysis. *SEG Expanded Abstracts* **28**, 835(2009)

Hansen, K., and Mittet, R. [2009] Incorporating seismic horizons in inversion of CSEM data. *SEG Expanded Abstracts* **28**, 694(2009).

Key, K., and Lockwood, A. [2009] Determining the orientation of marine CSEM receivers using orthogonal Procrustes rotation analysis. *Preprint 2009 (accepted for publication in Geophysics)*.

Mittet, R., Løseth, L., and Ellingsrud, S. [2004] Inversion of SBL data acquired in shallow waters. *66th EAGE Conference and Exhibition, Extended Abstracts*, E020.

Mittet, M., Aakervik, O. M, Jensen, H. R., Ellingsrud, S., and Stovas, A. [2007] On the orientation and absolute phase of marine CSEM receivers. *Geophysics* **72**, F145(2007)

Morten, J. P., Bjørke, A. K., Støren, T., Coward, E., Karlsen, S. A., and Roth, F. [2009a] Importance of azimuth data for 3D inversion of marine CSEM scanning data. *71st EAGE Conference and Exhibition*, *Extended Abstracts*, X005.

Morten, J. P., Bjørke, A. K., and Støren, T. [2009b] CSEM data uncertainty analysis for 3D inversion. *SEG Expanded Abstracts* **28**, 724(2009)

Roth, F., and Zach, J. J. [2007] Inversion of marine CSEM data using up-down wavefield separation and simulated annealing. *SEG Expanded Abstracts* **26**, 524(2007)

Zach, J. J., Bjørke, A. K., Støren, T., and Maaø, F. [2008a] 3D inversion of marine CSEM data using a fast finite-difference time-domain forward code and approximate hessian-based optimization. *SEG Expanded Abstracts* **27**, 614(2008).

Zach, J. J., Roth, F., and Yuan, H. [2008b] Data Preprocessing and Starting Model Preparation for 3D Inversion of Marine CSEM Surveys. *70th EAGE Conference and Exhibition*, *Extended Abstracts*, G003.

Zhu, C., Byrd, H., Nocedal, J. [1997] L-BFGS-B: Algorithm 778: L-BFGS-B, FORTRAN routines for large scale bound constrained optimization. *ACM Transactions on Mathematical Software* **23**, 550–560.